SIMPLIFIED ANALYTICAL MODELING OF DYNAMIC BEHAVIOR OF THE KEYHOLE FOR DIFFERENT SPATIAL LASER INTENSITY DISTRIBUTIONS DURING LASER DEEP PENETRATION WELDING*

J. VOLPP, M. GATZEN and **F. VOLLERTSEN**
BIAS — Bremer Institut fuer Angewandte Strahltechnik GmbH
2 Klagenfurter Str., 28359, Bremen, Germany. E-mail: volpp@bias.de

During laser deep penetration welding a characteristic keyhole is created, when the intensity of laser beam exceeds material depending limit. The generated system of keyhole and surrounding melt pool is highly dynamic. Dynamics in the weld pool and in keyhole are mainly responsible for keyhole instabilities that can cause keyhole collapses during the welding process. This can lead to unwanted enclosures or pores that reduce the quality of welded joint. For better understanding of the complex system, a simplified analytical model of the keyhole is used providing a description of the keyhole geometry. It also calculates the influence of different spatial laser intensity distributions on keyhole dynamics and resultant tendency to form pores. The model is used to calculate the temperature on the keyhole wall from energy equation containing laser beam energy absorption, heat conduction and evaporation losses. The surface temperature is needed to calculate the keyhole radius by solving the pressure equilibrium equation. This contains the recoil pressure at the end of the Knudsen layer on the keyhole surface, which keeps the keyhole open against the surface tension pressure of the surrounding liquid material. In the second step, a dynamic equation that describes the keyhole behavior is used. The dynamic calculation is based on the force balance in the keyhole. To observe the influence of different spatial laser intensity distributions the Gaussian and top hat distribution are implemented in calculation. It can be found that the keyhole geometry is influenced by different laser intensity distributions and pressure gradient changes significantly leading to highly different dynamic behaviors. 18 Ref., 2 Figures.

Keyword: *laser welding, deep penetration, keyhole, radiation intensity, spatial radiation, analytical model, keyhole geometry, weld metal, pore formation*

Pores are one of the failures occurring in laser deep penetration welding that reduce weld quality. Pores can be formed due to chemical reasons [1], laser power instabilities [2], changes in absorptivity or process instabilities [3]. Weld pool and keyhole dynamics can cause the keyhole to collapse. A high amplitude of the oscillating keyhole walls leads to a closing of the keyhole. Gas enclosures are formed usually in the lower part of the keyhole [4]. The captured gas cannot escape to the surface and forms a bubble in the weld pool. After solidification of the weld pool a pore is formed [5]. Although keyhole dynamics have been a field of interest and a lot of research has been done, the complex system is still not completely understood. Experimental observations found process oscillations in the range from 1 [6] to 8 kHz [7], and it was concluded that these high frequencies must origin from keyhole oscillations.

There were also mathematical approaches describing the process in the keyhole. In several former works numerical approaches were used to describe the complex system. Ki et al. [8] presented the model including all important known physical effects taking place in the keyhole and weld pool. For observing oscillations in kilohertz ranges, a numerical calculation requires small time steps and high calculation time [9]. Therefore, an analytical description is desired. Analytical models need shorter calculation times but require simplifications. It is, for example, not possible to solve the heat conduction equation for arbitrary shapes. Research has been done in analytical modeling of the keyhole for quasi-static calculations [10] as well as for dynamic behavior calculations [11]. Most former works used the Gaussian beam as a beam source for calculations. But industrially used laser sources provide quite different intensity distributions.

*Based on Proceedings of the 6th International Conference on Mathematical Modelling and Information Technologies in Welding and Related Processes (29 May–1 June, 2012, Katsiveli, Ukraine).

Kaplan [12] started to also consider the axial change of the intensity profile of the laser beam [13]. Not only the intensity value [14] and power oscillations [15] but also the spatial laser intensity distribution has been identified as being an influencing factor. The absorbed energy, temperature in the keyhole and pressure in it depend on the intensity and intensity profile of the beam [16]. Therefore, the influence of different intensity distributions of the laser beam are observed in this work with the aim of finding a way to reduce pores.

Based on these existing analytical models the influence of the Gaussian and top hat laser intensity distribution on keyhole geometry [10] and dynamics [11] is observed to obtain a better understanding of the keyhole process.

Analytical model of the keyhole. *Modeling quasi-static keyhole*. When the keyhole has formed due to high intensity of the laser beam a quasi-static condition is achieved. A cylindrical keyhole for thin sheets can be assumed that is completely penetrating the material. The macroscopic shape is conserved when the beam is moved relatively to the material. Due to the vaporization process an ablation or recoil pressure p_{abl} in the keyhole is built up that opens the keyhole and counteracts against the pressure of the surface tension p_γ of the surrounding melt pool. Mathematically the pressure balance equation can be expressed as

$$\Delta p = p_\gamma - p_{\text{abl}}. \tag{1}$$

Hydrodynamic and hydrostatic pressures can be neglected [17] as their dimension is much smaller than the one of the surface tension calculated with the Laplace description:

$$p_\gamma = \frac{\gamma}{r_{\text{kap}}}. \tag{2}$$

Surface tension pressure depends on the radius r_{kap} and the surface tension coefficient γ.

The ablation pressure p_{abl}, caused by vaporization of material on the keyhole wall in the so called Knudsen layer, can be calculated as

$$p_{\text{abl}} = mn(T_{\text{s}})u^2(T_{\text{s}}), \tag{3}$$

where m is the atomic mass; n is the particle density; u is the velocity of evaporated particles. Particle density and velocity of evaporated particles are dependent on keyhole surface temperature T_{s} that can be calculated solving the energy equation as

$$q_{\text{abs}} = q_\lambda + q_{\text{abl}}. \tag{4}$$

The absorbed part of the energy q_{abs}, provided by the laser beam, can be calculated using

$$q_{\text{abs}} = \frac{1}{2\pi rd} \int i(r) r dr d\varphi, \tag{5}$$

where d is the sheet thickness; r and φ is the radial and azimuthal coordinate. Laser intensity distribution i in this equation is the parameter that can be varied.

Energy losses are mainly vapor losses ablating from the keyhole

$$q_{\text{abl}} = mn(T_{\text{s}})u(T_{\text{s}})H_{\text{v}} \tag{6}$$

and heat conduction losses

$$q_\lambda = \frac{T_{\text{s}} - T_0}{2} \rho c_p u_0 K_1(\text{Pe}) / K_0(\text{Pe}). \tag{7}$$

Here H_{v} is the latent heat; T_0 is the ambient temperature; ρ is the density of the liquid material; c_p is the heat capacity; u_0 is the welding speed; K_1 and K_0 is the modified Bessel functions of first and zero order depending on the Peclet number $\text{Pe} = u_0 r_{\text{kap}} / 2\kappa$, where κ is the thermal diffusivity. Equation (7) is the solution of the heat conduction equation describing losses through heat conduction assuming a simplified cylindrical heat source [10].

Calculating the surface temperature T_{s} at the wide range of radii, the pressure equilibrium equation $\Delta p = 0$ can be solved, and quasi-static radii of the cylindrical keyhole can be determined.

Modeling dynamic behavior of the keyhole. To model the dynamic behavior of the keyhole differential equations are necessary. The cylindrical keyhole calculated above is assumed to oscillate only in the radial direction, and the intensity distribution is the parameter in the model. Including the composition of all forces F acting in the keyhole, the dynamic equation of radius can be written as follows:

$$\ddot{r} = \dot{b} = \frac{F}{m_{\text{m.p}}}, \tag{8}$$

where $\ddot{r}$ is the radius normalized (to the beam radius) keyhole radius; $\dot{b}$ is the rate of radius change; $m_{\text{m.p}}$ is the melt pool mass. According to [11] the dynamic equation of velocity $\dot{b}$ is

$$\dot{b} = 2\pi d(rp + 1) + 12\pi \frac{d^2}{r_0^2} r \times \times \frac{(1 - r^2)}{(c - r)^2 (c^2 - r^2)} - fb, \tag{9}$$

where c is the factor that accounts for the acceleration due to melt pool deformation at the top surface. First and second term in (9) describe velocities induced by ablation pressure, surface tension and melt pool deformation at the surface. The last term accounts for the viscous velocity dissipation, where f is the dissipation factor that causes damping of the system.

The dynamic pressure is described by [11]

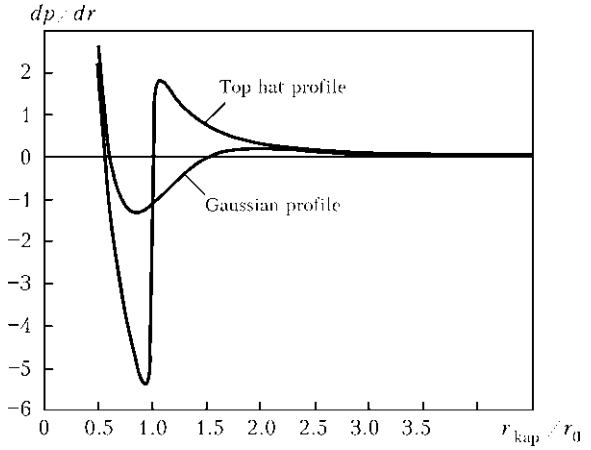

Figure 1. Pressure gradient for the Gaussian and top hat laser profile

$$\dot{p} = \sqrt{\frac{m_{\text{m.p}}}{\gamma}} \times \tag{10}$$

$$\times \left(2\frac{v_{\text{a}}}{d}\left(\frac{p_0}{p_{\text{eq}}} - p\right) + \frac{c_0}{\pi d p_0 r_0^2 r^2}\, i(r,\, r_{\text{kap}},\, r_0) - 2p_0 r_{\text{kap}}^2 \frac{b}{r^3} \right).$$

Here $\dot{p}$ is the pressure in the keyhole normalized to the quasi-static equilibrium pressure p_{eq}. The first part of the right hand side of (10) describes the pressure change due to vapor escaping through keyhole opening, where v_{a} is the the assumed velocity of the exiting vapor; p_0 is the ambient pressure. The pressure change due to laser evaporation is found in the second term, where c_0 is the constant relating to laser power; r_0 is the beam radius. The third term in (10) describes the pressure change due to adiabatic volume change of the keyhole. This set of differential equations can be solved, and the response on special perturbations can be calculated.

Evaluation. For evaluating the model, two different laser intensity profiles are examined. First, the Gaussian beam is considered:

$$i_{\text{Gs}}(r) = \frac{P_{\text{abs}}}{\pi r_0^2}\, e^{-(r/r_0)^2}, \tag{11}$$

second, the top hat profile is used:

$$i_{\text{t.h}}(r) = \frac{P_{\text{abs}}}{\pi r_0^2}\left(\frac{1}{2} - \frac{1}{\pi}\,\text{arctg}\left(\frac{r - r_0}{\alpha}\right)\right), \tag{12}$$

where P_{abs} is the abrorbed laser power; α is the factor determining the steepness of the function.

Mathworks® Matlab (Vers. R2009a) is used to calculate the quasi-static keyhole geometry, and Simulink (Vers. 7.3) is used to calculate the dynamic behavior of the keyhole geometry and pressures. For the culations the set of following typical parameters is used: P_{abs} = 900 W; r_0 = = 100 μm; α = 1 μm; u_0 = 1 m/min; d = 1 mm; c_0 = 0.2; f = 0.1; c = 3; v_a = 4 m/s; r_{start} = 1.2; p_{start} = 1. Radius r_{start} and pressure p_{start} are normalized to calculated quasi-static values of radius and pressure.

Results of modeling. *Quasi-static keyhole*. For the Gaussian and top hat profile, the pressure gradient for the wide range of r_{kap} normalized to r_0 is calculated (Figure 1).

Both curves equal zero 2 times, but only the second zero is stable. A small deviation of the first zero would lead to a collapse of the keyhole. The resulting keyhole radius obtained by the Gaussian beam is slightly smaller than that produced by the top hat distribution. Although the radius is similar, the restoring forces are different. The forces can be correlated to the pressure gradient when the radius deviation occurs. Figure 1 shows that higher pressure gradient is calculated for the top hat than for Gaussian beam.

Dynamic behavior. Different restoring forces in the keyhole of different incident laser beams lead to different dynamic behavior. Both radii are deviated, and the dynamic behavior is calculated by the model. Time t has to be normalized to

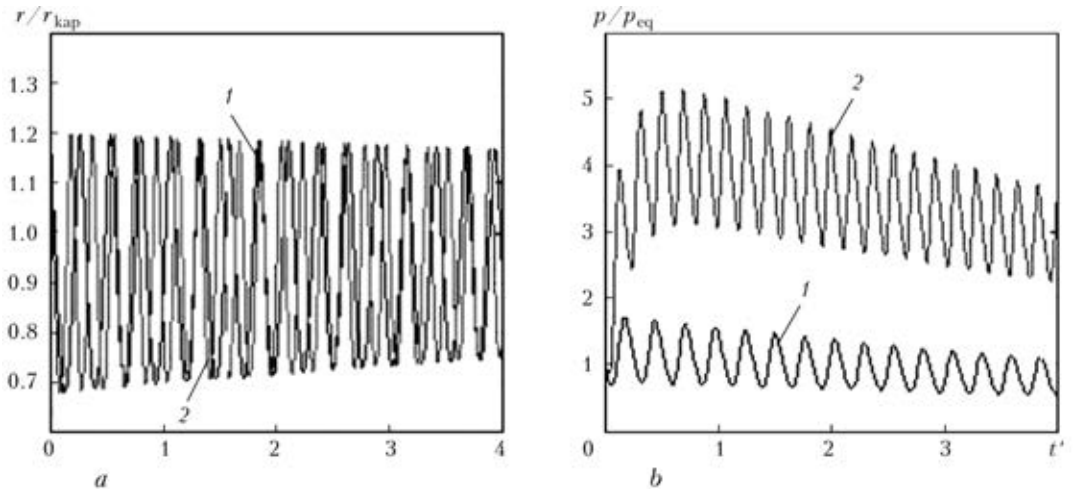

Figure 2. Keyhole radius (*a*) and pressure (*b*) oscillations for the Gaussian (*1*) and top hat (*2*) laser intensity distribution

$$t' = t\sqrt{\frac{m_{\text{m.p}}}{\gamma}}. \quad (11)$$

Figure 2, *a* shows the oscillating radius around the equilibrium with different frequencies for different intensity distributions. They are found to be approximately 1.6 and 3.2 kHz for the Gaussian and top hat intensity distribution, respectively.

In Figure 2, *b* the pressure balance is shown. Pressure rises in both cases to different starting values and oscillates with different frequencies for different incident beams. Down slope of the curves is caused by the damping of the oscillation by surrounding material.

Results. It can be seen from the results of the modeling that different spatial laser intensity distributions have different effects on both keyhole geometry and dynamics. Impact on the keyhole pressure and also the keyhole radius is rather small. Radial dependency of the pressure gradient is much more significant. Particularly the explicit steepness of the intensity change with radius for the top hat distribution is assumed to cause a notably higher pressure gradient in the region of the stable quasi-static keyhole radius. As the pressure gradient influences the force balance, different dynamic behaviors are expected for different spatial laser intensity distributions. Fabbro et al. [18] was able to measure these pressure oscillations resulting from radius dynamics. The frequency of pressure and radius oscillations are especially influenced by different beam profiles. The higher frequency for the top hat distribution can be explained by the higher amplitude of the pressure oscillation that results in a stronger restoring force and, hence, higher velocities. This also results from the higher radial pressure gradients caused by the top hat distribution. Found frequency values are in the same range as they were experimentally measured in works [6] or [7]. It seems that the top hat distribution is more beneficial to producing stable keyhole than the Gaussian beam. Recoil pressure seems to damp the oscillations much more quickly that leads to smaller influence of the surrounding melt pool. Higher pressure gradient seems to inhibit the keyhole collapse.

Conclusion

Using the analytical model for calculating quasi-static keyhole and dynamic behavior, the effect of different spatial laser intensities on the keyhole geometry and dynamics can be shown. Calculations of the used model show small influence of the different laser intensity profiles on keyhole geometry. Higher pressure gradient is calculated for the top hat intensity distribution than for the Gaussian beam. For the observed radius perturbation different oscillation frequencies and amplitudes are found for the top hat and Gaussian intensity profile due to different pressure gradients. Using this model the top hat distribution seems to result in more stable keyhole.

Acknowledgements. *The authors appreciate the funding of the Project VO 530/40-1 from DFG (Deutsche Forschungsgemeinschaft) sincerely.*

1. Tsukamoto, S., Arakane, G., Kojima, K. et al. (2007) Effect of alloying elements on porosity formation in laser welding of heavy section steel plates. *IIW Doc. IV-941–07*.
2. Szymanski, Z., Hoffman, J., Kurzyna, J. (2001) Plasma plume oscillations during welding of thin metal sheets with a CW CO_2 laser. *J. Phys. D: Appl. Phys.*, **34**, 189–199.
3. Matsunawa, A., Kim, J.D., Katayama, S. et al. (1996) Experimental and theoretical studies on keyhole dynamics in laser welding. In: *15th ICALEO Proc.* (14–17 Oct. 1996, Detroit, USA), **81**, 58–67.
4. Berger, P., Hugel, H., Graf, T. (2011) Understanding pore formation in laser beam welding. *Physics Procedia*, **12**, 241–247.
5. Liu, L., Song, G., Liang, G. et al. (2005) Pore formation during hybrid laser-tungsten inert gas arc welding of magnesium alloy AZ31B — Mechanism and remedy. *Materials Sci. and Eng. A*, **390**, 76–80.
6. Semak, V., Hopkins, J., McCay, M. et al. (1995) Melt pool dynamics during laser welding. *J. Phys. D: Appl. Phys.*, **28**, 2443–2450.
7. Klassen, M. (2000) *Prozessdynamik und resultierende Prozessinstabilitaeten beim Laserstrahlschweissen von Aluminiumlegierungen*: PhD thesis, University of Bremen.
8. Ki, H., Mohanty, P., Mazumder, J. (2002) Modeling of laser keyhole welding. Pt I: Mathematical modeling, numerical methodology, role of recoil pressure, multiple reflections, and free surface evolution. *Metallurg. and Mater. Transact.*, **33**, June.
9. Pitz, I., Otto, A., Schmidt, M. (2011) Accelerated simulation of laser beam forming by means of moving meshes. In: *IWOTE Proc.* (Bremen, April 6–7, 2011).
10. Kroos, J., Gratzke, U., Simon, G. (1993) Towards a self-consistent model of the keyhole in penetration laser beam welding. *J. Phys. D: Appl. Phys.*, **26**, 474–480.
11. Pleteit, H. (2001) *Analyse und Modellierung der Keyhole-Dynamik beim Laserstrahlschweissen von Aluminiumlegierungen*: PhD thesis, University of Bremen.
12. Kaplan, F. (2011) Influence of the beam profile formulation when modeling fiber-guided laser welding. *J. Laser Appl.*, 23(**4**), Nov.
13. Marten, O., Wolf, S., Hansel, K. et al. (2010) Qualifizierung von Fokussier- und Abbildungssystemen fur die industrielle Laserbearbeitung mit brillanten Strahlquellen im Multikilowattbereich. In: *Laser-Anwenderforum Proc.* (Bremen, 24–25 Nov., 2010).
14. Khan, M., Romoli, L., Dini, G. et al. (2011) A simplified energy-based model for laser welding of ferritic stainless steels in overlap configurations. *CIRP Annals E*, 60(**1**), 215.
15. Schmidt, M., Otto, A., Kageler, C. et al. (2008) Analysis of YAG laser lap-welding of zinc coated steel sheets. *Ibid.*, 57(**1**), 213.
16. Hugel, H., Graf, T. (2009) *Laser in der Fertigung: Strahlquellen, Systeme, Fertigungsverfahren*. Stuttgart: Vieweg+Teubner.
17. Klein, T., Vicanek, M., Kroos, J. et al. (1994) Oscillation of the keyhole in penetration laser beam welding. *J. Phys. D: Appl. Phys.*, 27(**10**), 2023–2030.
18. Fabbro, R., Slimani, S., Coste, F. et al. (2005) Study of keyhole behaviour for full penetration Nd: YAG CW laser welding. *Ibid.*, **38**, 1881–1887.

Received 16.01.2013